Journal of Materials Science: Materials in Electronics (2019) 30:5929–5935
https://doi.org/10.1007/s10854-019-00892-2

Thermoelectric performance of skutterudite $Ni_xCo_{4-x}Sb_{12}$ rapidly synthesized by microwave heating

Ying Lei[1,4] · Leiqiang Ma[1] · Rui Zheng[1] · Yu Li[1] · Rundong Wan[2] · Wen Chen[3] · Hongwei Zhou[4] · Wensheng Gao[1]

Received: 18 October 2018 / Accepted: 5 February 2019 / Published online: 12 February 2019

Abstract
In the present work, a series of single phase Ni-doped skutterudite compounds $Ni_xCo_{4-x}Sb_{12}$ (x = 0.1, 0.2, 0.3, 0.4, 0.5) were successful synthesized by 5 min microwave heating for the first time. The resulting ingots was pulverized and sintered by spark plasma sintering to fabricate bulk samples, and their microstructure and thermoelectric properties have been investigated systematically. The results show that the matrix grain characteristics are influenced by Ni concentration and microwave irradiation. The $Ni_{0.3}Co_{3.7}Sb_{12}$ bulk has the smallest and uniform grain size of about 1–2 μm. The maximum power factors of $Ni_xCo_{4-x}Sb_{12}$ are 2273, 2479, 2711, 2613 and 2526 $\mu Wm^{-1}K^{-2}$ respectively. A highest ZT of 0.52 for $Ni_{0.3}Co_{3.7}Sb_{12}$ is achieved at 773 K along with a total thermal conductivity of 3.8 $Wm^{-1}K^{-1}$.

1 Introduction

Thermoelectric (TE) conversion technology could directly convert waste heat into electricity based on the Seebeck effect, which can become an important part of the solution to today's ever-increasing energy and environmental crisis [1]. The application of thermoelectric conversion technology depends on the development of thermoelectric materials which requires the optimization of thermal and electrical transportation to achieve a high thermoelectric figure of merit (ZT), defined as $ZT = S^2T/\rho\kappa$, where S, ρ and κ is the Seebeck coefficient, electrical conductivity and thermal conductivity, respectively. Excellent TE materials should have good electrical and thermal transport properties simultaneously, namely, as high as possible Seebeck coefficient and as small as possible electronic thermal conductivity and lattice thermal conductivity.

Skutterudites, body-centered cubic structure AB_3 (A: Co, Rh, Ir; B: P, As, Sb) compounds, are widely recognized as promising medium-temperature thermoelectric materials because they can satisfy the phonon-glass and electron-crystal scattering concept [2–4]. In the family of skutterudite compounds, $CoSb_3$-based material is of the most interest to researchers due to their good electronic properties and stable mechanical property. Nevertheless, pure $CoSb_3$ cannot be used in thermoelectric applications because its electrical resistivity and especially thermal conductivity are very high [3]. Two approaches, *i.e.*, filling impurity atom into intrinsic holes or doping treatment [5–8], could be used to improve the thermal and electrical transport property of $CoSb_3$-based materials. It is well known that Ni-doping in $CoSb_3$-based skutterudites not only controls the conduction type but also enhances ZT through reduction of both electrical resistivity and thermal conductivity [3, 9–16]. Kitagawa et al. [12], Il-Ho et al. [13], Soon-Chul et al. [14] and Qinyu et al. [15] reported ZT of 0.28 (600K), 0.2 (650K), 0.3 (650K) and 0.7 (823K) for $Co_{0.95}Ni_{0.05}Sb_3$, $Co_{0.9}Ni_{0.1}Sb_3$, $Co_{0.93}Ni_{0.07}Sb_3$ and nanostructured $Co_{0.91}Ni_{0.09}Sb_3$ enhanced by Ni-doped, respectively. Ahmad et al. [16] reported largest power factor

✉ Yu Li
liyuahut@163.com

✉ Rundong Wan
rdwan@kmust.edu.cn

✉ Wen Chen
chen_wen@vip.sina.com

[1] School of Metallurgical Engineering, Anhui University of Technology, Maxiang Road, Ma'anshan 243032, China

[2] College of Materials Science and Engineering, Kunming University of Science and Technology, 727 South Jingming Road, Chenggong New District, Kunming 650093, China

[3] Institute of Mineral Resources Development and Utilization, Changsha Research Institute of Mining and Metallurgy CO., LTD, 966 South Lushan Road, Changsha 410012, China

[4] State Key Laboratory of Advanced Processing and Recycling of Nonferrous Metals, Lanzhou University of Technology, 287 Langongping Road, Lanzhou 730050, China

value of 13.65 μW/cm-K^2 for $Co_{3.922}Ni_{0.078}Sb_{12}$ at 475 K, 25 times improvement over the non-doped $CoSb_3$.

The skutterudite compounds powder or ingot is usually synthesized *via* smelting [12–14], mechanical alloying [15], wet synthesis [16], or solid-state reaction [17–19]. Then the resulting powder or ingot is quenched, annealed for several days and subsequently sintered with spark plasma sintering or hot press sintering to fabricate bulk thermoelectric materials. The conventional fabrication techniques are complex and inefficient, so it's important to explore new synthetic method which could lead to the superior thermoelectric compounds with better structural and performance. Microwave heating techniques, possessing characteristics of instantaneous, volumetric and selective heating, might offer faster and cost-effective processes for synthesis reaction [20–26]. In the present work, a series of Ni-doped skutterudite $Ni_xCo_{4-x}Sb_{12}$ (x = 0.1, 0.2, 0.3, 0.4, 0.5) bulks were fabricated by combination of microwave synthesis and spark plasma sintering (SPS). The phase composition, grain growth characteristics and thermoelectric performance were investigated. The effects of the microwave heating and impurity on microstructure and thermoelectric properties were systematically studied.

2 Experimental

The starting metal powders are nickel (Ni, ~48 μm, 99.9%, Aladdin), cobalt (Co, ~48 μm, 99.99%, Aladdin) and antimony (Sb, ~20 μm, 99.9%, Aladdin). The three powders were weighed and mixed at nominal compositions of $Ni_xCo_{4-x}Sb_{12}$ (x = 0.1, 0.2, 0.3, 0.4, 0.5) and subsequently formed as button on powder compressing machine. The resulting button was sealed in vacuumed quartz tube and subsequently heated in microwave oven for 5 min (M1-L202B/700W, Midea/China). The synthesized ingot was pulverized and sintered by spark plasma sintering (SPS) (LABOX-100, Sinter Land INC./Japan) at 903 K for 5 min to fabricate bulk sample. More details concerning the process used are described in our previous papers [24–26].

The phase composition for bulk samples was detected by X-ray diffraction (XRD) on Bruker/D8-ADVANCE diffractometer with Cu-Kα radiation (λ = 1.54 Å) and scanning speed of 1 degree per min. The microstructure was observed by field emission scanning electron microscope (FE-SEM) on FEI/Nano-SEM430. The Seebeck coefficient and electrical resistivity were tested on JouleYacht/Namicro-3 test system at the range from room temperature to 773K with a step of 25 K. The thermal diffusivity was measured on Netzsch/LFA-427 laser flash thermal analyzer at the range from room temperature to 773K with a step of 100 K, then the thermal conductivity was calculated as $\kappa = DdC_p$, where D is the thermal diffusivity, d is the sample density determined basing on the Archimedes' method, C_p is the temperature dependence specific heat capacity, for $CoSb_3$-based compounds whose value could be estimated as 0.24 J·g^{-1}·K^{-1} [27].The electronic thermal conductivity was calculated as $\kappa_{el} = LT/\rho$, where ρ is electrical resistivity, L is Lorenz number estimated as $2.0 \times 10^{-8} V^2K^{-2}$ [6]. The lattice thermal conductivity was calculated as $\kappa_{lat} = \kappa - \kappa_{el}$. The thermoelectric figure of merit was calculated as $zT = T \times (S^2\sigma)/\kappa$.

3 Results and discussion

3.1 Microstructures

The XRD patterns of $Ni_xCo_{4-x}Sb_{12}$ compounds after SPS are shown in Fig. 1. All samples are single phase in accordance with the standard PDF card of $CoSb_3$. Because the sintering temperature of 903K cannot meet the demand of alloying reaction, we vary the phase compositions of $Ni_xCo_{4-x}Sb_{12}$ through controlling the microwave synthesis process. Nearly single phase of different types of thermoelectric compounds, e.g., $CoSb_3$, TiNiSn, CuSe, BiCuSeO, were achieved in 1–5 min microwave synthesis [24–26, 28–31]. As the inset in Fig. 1 shows that the XRD peak (310) of $Ni_xCo_{4-x}Sb_{12}$ compounds shift towards higher angles, indicating that Ni successfully enters into the Co site.

The lattice constants of $Ni_xCo_{4-x}Sb_{12}$ were calculated by using MDI Jade 5.0 software (DELL/Materials Date, Inc.) basing on the XRD patterns. It can be seen from Fig. 2 that the Ni doping causes a decrease of lattice parameter due to the relative smaller radius of nickel (~1.62 angstrom) atom than that of cobalt (~1.67 angstrom) atom. The lattice parameters of $Ni_xCo_{4-x}Sb_{12}$ basically decrease with the increase of Ni concentration. The

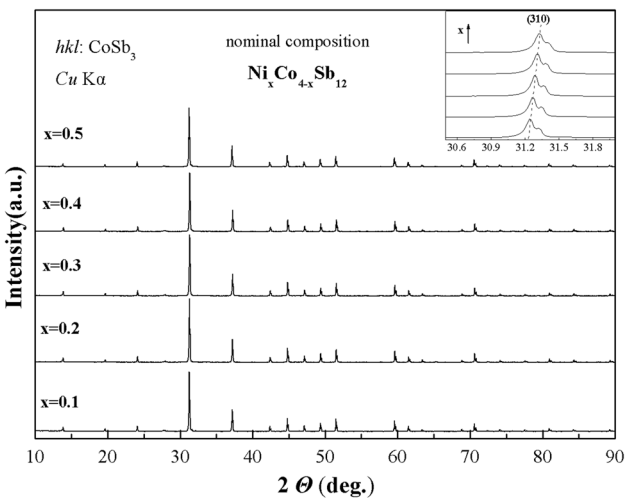

Fig. 1 Powder XRD patterns of $Ni_xCo_{4-x}Sb_{12}$ compounds

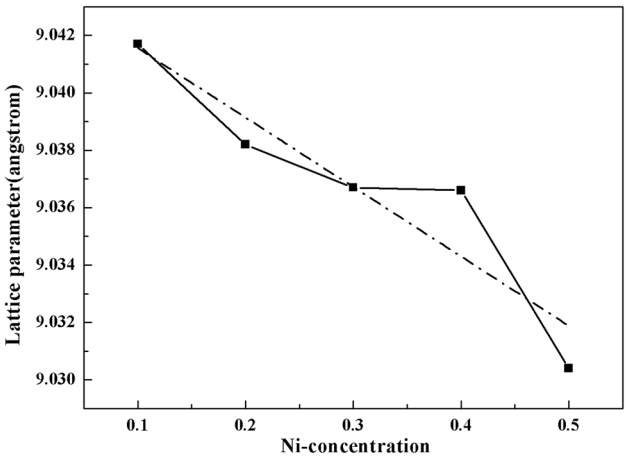

Fig. 2 Lattice parameters of $Ni_xCo_{4-x}Sb_{12}$ compounds

lattice parameter depends on the real composition which is related to the reaction state of the synthesis process. The lattice parameters of $Ni_{0.3}Co_{3.7}Sb_{12}$ and $Ni_{0.4}Co_{3.6}Sb_{12}$ are not so different, meaning that the real compositions for them are close to each other. The possible reason is that the reaction states of different samples are not exactly the same due to the ultra-fast reaction rate of microwave synthesis. The lattice parameters calculated in this work are similar with those of samples obtained by conventional method [16].

The real densities of $Ni_xCo_{4-x}Sb_{12}$ compounds (x = 0.1, 0.2, 0.3, 0.4, 0.5) are measured as 7.554, 7.550 7.540, 7.557 and 7.597 respectively based on Archimedes' method. The FE-SEM morphologies of cross section of $Ni_xCo_{4-x}Sb_{12}$ bulks are shown in Fig. 3a–e. The matrix grain and the grain boundaries are clearly visible in the field of view. The matrix grain sizes of $Ni_xCo_{4-x}Sb_{12}$ are about 1 to several micrometers with varying degrees of unevenness. The insets show the details of matrix grain for $Ni_xCo_{4-x}Sb_{12}$ bulks. The $Ni_{0.1}Co_{3.9}Sb_{12}$ sample and $Ni_{0.3}Co_{3.7}Sb_{12}$ sample obviously have the maximum and minimum grain size, respectively. The decreasing order of grain sizes for $Ni_xCo_{4-x}Sb_{12}$ (0.1, 0.2, 0.3, 0.4, 0.5) are $Ni_{0.1}Co_{3.9}Sb_{12}$ (maximum), $Ni_{0.2}Co_{3.8}Sb_{12}$ and $Ni_{0.4}Co_{3.6}Sb_{12}$, $Ni_{0.5}Co_{3.5}Sb_{12}$, $Ni_{0.3}Co_{3.7}Sb_{12}$ (minimum). From the above, it can be deduced that the grain sizes for $Ni_xCo_{4-x}Sb_{12}$ depend on not only the point defects introduced by Ni doping, but also the microwave synthesis process. It is generally believed that the higher the heating rate the finer the grain size, however, it's hard to control the grain size precisely in microwave field. The EDS elemental distribution maps of $Ni_{0.3}Co_{3.7}Sb_{12}$ bulk are shown in Fig. 4. The results show that the concentration and distribution of Ni, Co and Sb coincide with the nominal composition of $Ni_{0.3}Co_{3.7}Sb_{12}$.

3.2 Electrical transport properties

The electrical resistivity, Seebeck coefficient and power factor of $Ni_xCo_{4-x}Sb_{12}$ compounds are shown in Fig. 5a–c. The most significant trend is that the electrical resistivity decreases with the increased Ni concentration due to the increase of free electron. The electrical resistivity of $Ni_{0.1}Co_{3.9}Sb_{12}$ decreases with the increased temperature due to the valence electrons constantly excited, exhibiting typical semiconductor behaviors. With the increase of Ni concentration, $Ni_xCo_{4-x}Sb_{12}$ gradually shows hybrid natures of semimetal and semiconductor behaviors, the electrical conductivity is very little affected by temperature, resulting in the very little variation of electrical resistivity. Similar trends can be seen in the previous works [15, 16].

The absolute value of Seebeck coefficients of $Ni_xCo_{4-x}Sb_{12}$ strictly decreases with the increased Ni concentration due to increase of electrical conductivity. There are maxima in the Seebeck coefficient *vs* temperature plots. The absolute value of Seebeck coefficient are firstly increase due to the reduction of chemical potential, which is a common phenomenon among degenerate semiconductors. With the increase of temperature, the lattice vibration will increase and resulting in significant enhancement of intrinsic excitation, and consequently cause the rapid increase of carrier concentration and decrease of Seebeck coefficient. Because of the bipolar effect, when at lower temperatures, the intrinsic excitation can be ignored and the carrier is mainly provided by the ionization of impurities (Se doping); on the opposite, when at higher temperatures, the intrinsic carriers dominate. The maximum Seebeck coefficients of $Ni_xCo_{4-x}Sb_{12}$, where x is 0.1, 0.2 ,0.3 0.4 and 0.5, are − 254, − 211, − 191, − 188 and −160 μVK^{-1}, respectively.

The variations of power factors for different Ni-doped samples are consistent, which firstly increase and then decrease with the increased temperature. The variations of power factors with the increase of Ni concentration for different samples are not regular. The main reason is that the power factors are proportional to the Seebeck coefficient and inversely proportional to the conductivity synchronously, high power factor are required for moderate electrical conductivity and relative high Seebeck coefficient. The maximum power factors of $Ni_xCo_{4-x}Sb_{12}$ are 2273, 2479, 2711, 2613 and 2526 $\mu Wm^{-1}K^{-2}$ respectively.

Overall, the electrical transport properties for un-filled $CoSb_3$ are sensitive to the Ni-doped concentration, which indicates that Ni atoms act as electron donors could significantly improve electrical conductivity at the cost of part of Seebeck coefficient, making the achieved power factors significantly higher than those of samples reported in previous works [16].

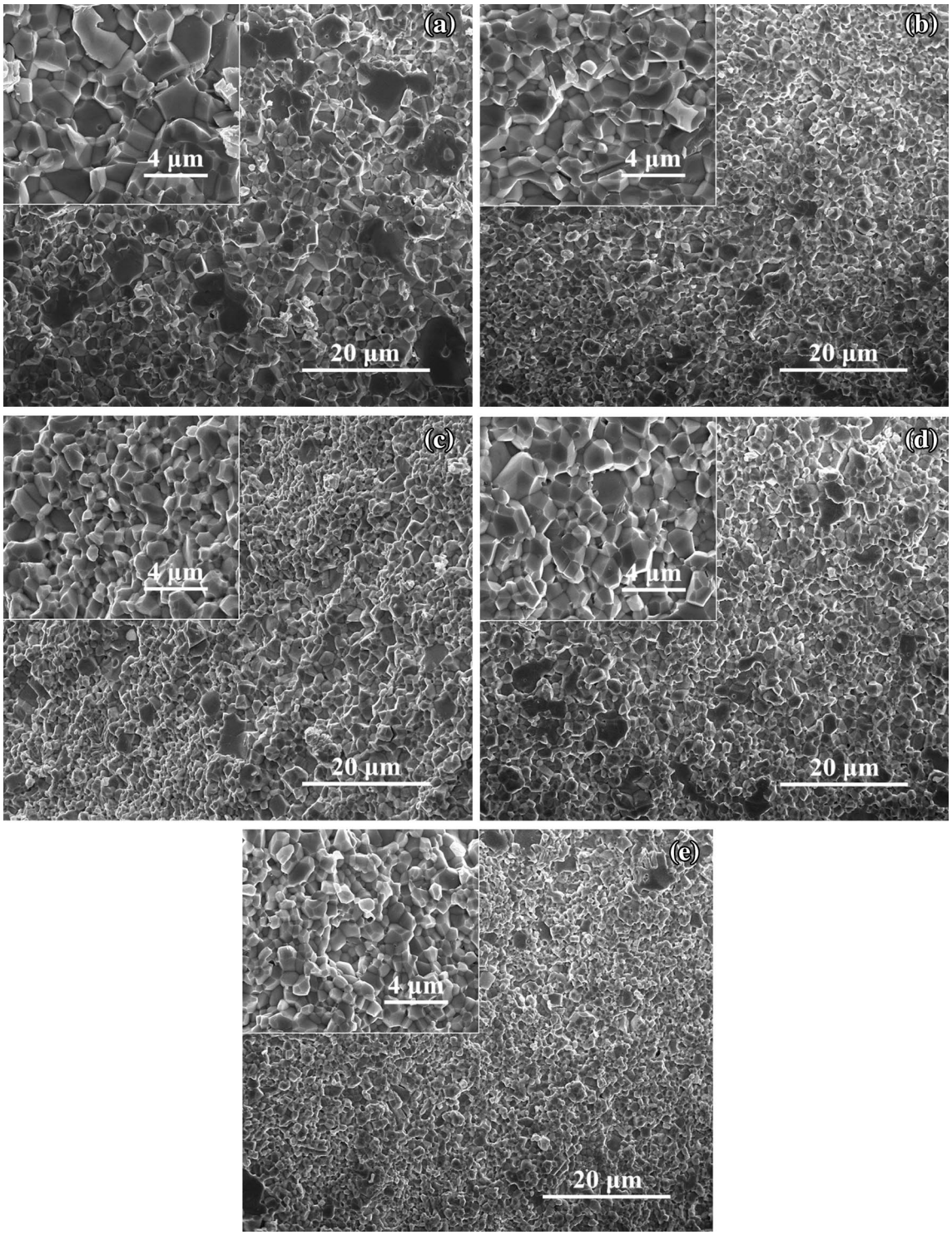

Fig. 3 FE-SEM morphology of cross section of $Ni_{0.1}Co_{3.9}Sb_{12}$ (**a**), $Ni_{0.2}Co_{3.8}Sb_{12}$ (**b**), $Ni_{0.3}Co_{3.7}Sb_{12}$ (**c**), $Ni_{0.4}Co_{3.6}Sb_{12}$ (**d**), $Ni_{0.5}Co_{3.5}Sb_{12}$ (**e**), respectively

3.3 Thermal transport properties

The temperature dependences of electronic thermal conductivity, lattice thermal conductivity and total thermal conductivity of $Ni_xCo_{4-x}Sb_{12}$ compounds are shown in Fig. 6a–c respectively. The electronic thermal conductivities increase with the increased Ni concentration due to the increase of electrical conductivity if the Lorenz is fixed. The

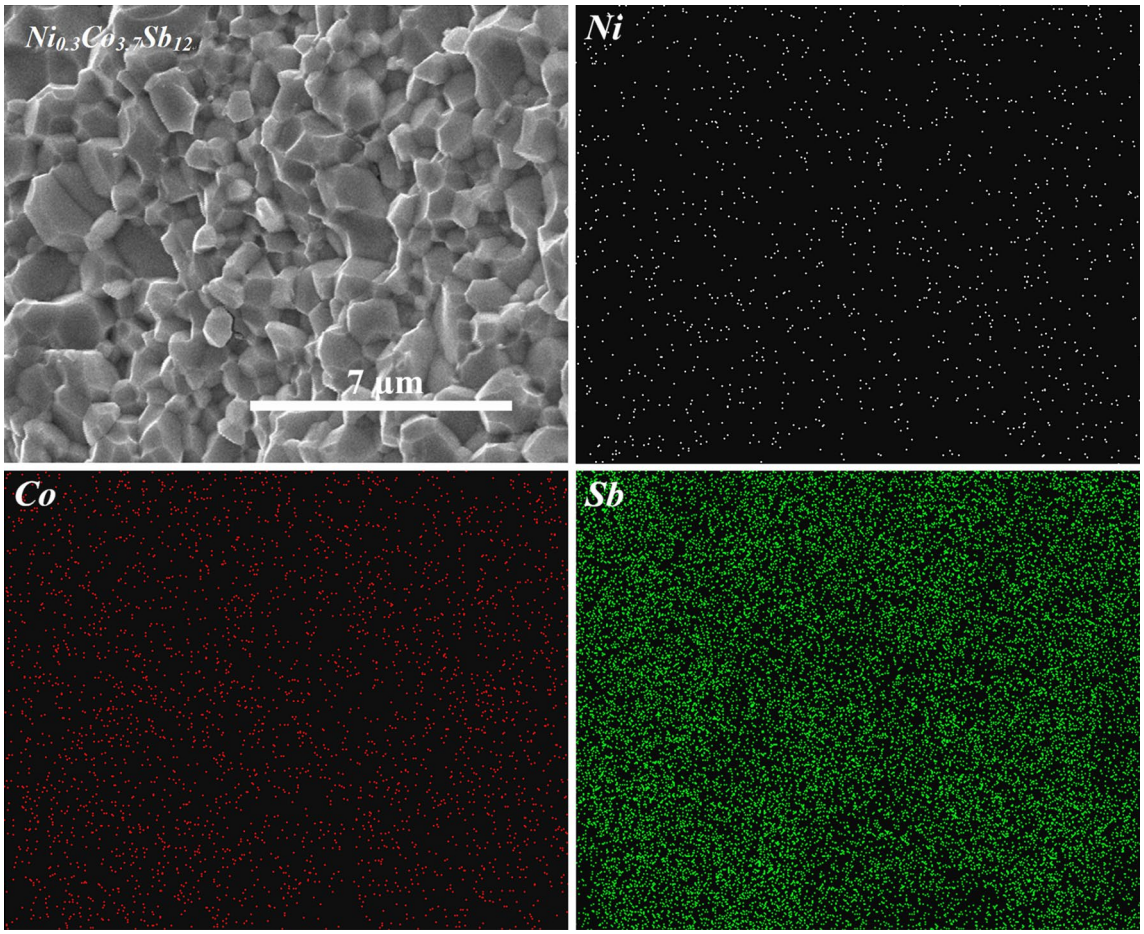

Fig. 4 EDS elemental distribution maps of $Ni_{0.3}Co_{3.7}Sb_{12}$ bulks

lattice thermal conductivities of $Ni_xCo_{4-x}Sb_{12}$ depend on the Ni concentration and the grain boundary characteristic. The lattice thermal conductivities at room temperature basically increase with the increased Ni concentration due to the increase of point defect. The lattice thermal conductivities are also influenced by the average grain size especially at relative higher temperature. The $Ni_{0.3}Co_{3.7}Sb_{12}$ bulk has the smallest lattice thermal conductivity of $2.73 Wm^{-1}K^{-1}$ at 773K, which is significantly smaller than those of un-filled samples synthesized by conventional ways [10, 12–14, 16]. The lattice thermal conductivity makes major contribution to the total thermal conductivity. The variation of total thermal conductivity is similar to that of lattice thermal conductivity due to the ambipolar diffusion. The total thermal conductivity of $Ni_{0.3}Co_{3.7}Sb_{12}$ is 3.89–5.56 $Wm^{-1}K^{-1}$.

3.4 Thermoelectric figure of merit, *ZT*

The thermoelectric figures of merit of $Ni_xCo_{4-x}Sb_{12}$ bulks are shown in Fig. 7. The thermoelectric figures of merit increase with the increased temperature. The $Ni_{0.3}Co_{3.7}Sb_{12}$ has the maximum ZT of 0.52 at 773 K and that the values larger might be realized at a bit higher temperature. The maximum ZT of 0.52 for the present sample synthesized *via* 5 min microwave heating is slightly smaller than that of nanostructured sample synthesized *via* 20–50 h mechanical alloying [15], but significantly greater than those of samples synthesized *via* smelting [12–14] and solid-state reaction [10].

4 Conclusions

In summary, a series of single phase Ni-doped skutterudite compounds $Ni_xCo_{4-x}Sb_{12}$ (x = 0.1, 0.2, 0.3, 0.4, 0.5) were successful synthesized by 5 min microwave heating for the first time. The $Ni_{0.3}Co_{3.7}Sb_{12}$ bulk has the smallest and uniform grain size of about 1–2 μm, such grain characteristic may beneficial to reduce the lattice thermal

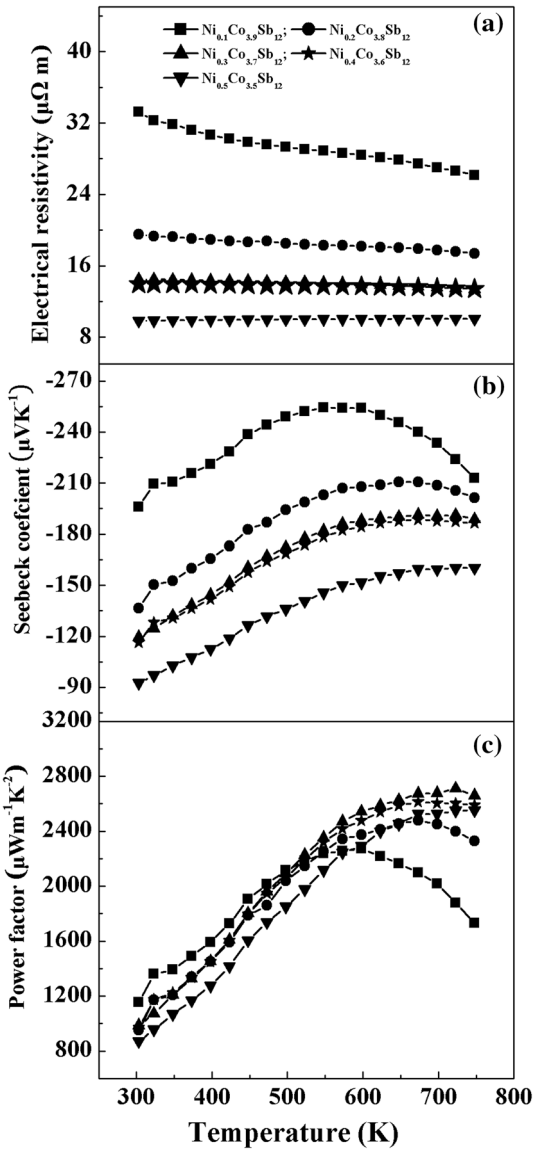

Fig. 5 Temperature dependences of electrical resistivity (**a**), Seebeck coefficient (**b**) and power factor (**c**) of $Ni_xCo_{4-x}Sb_{12}$ bulks, respectively

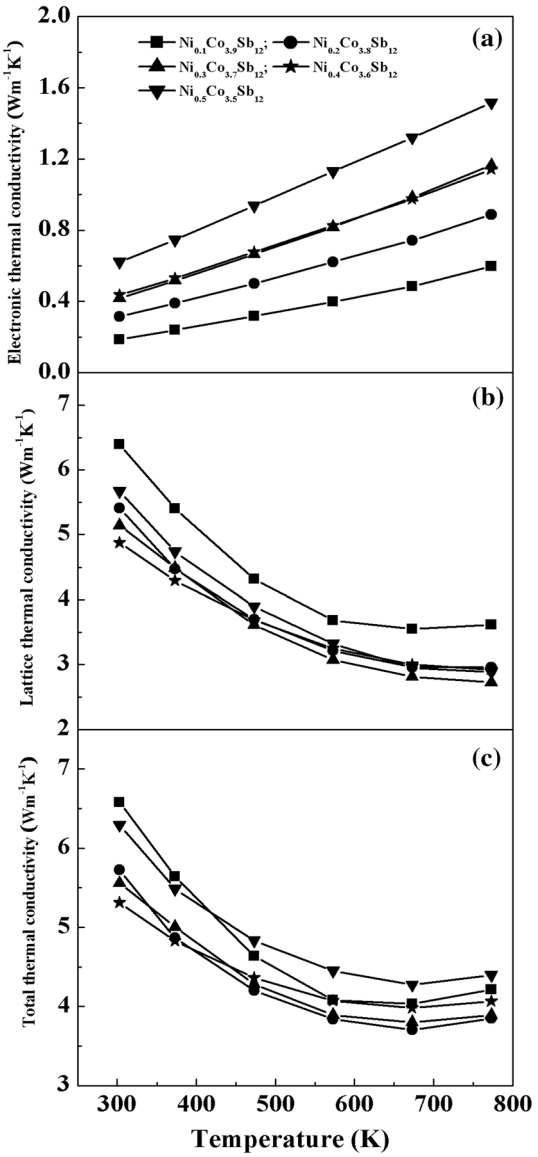

Fig. 6 Temperature dependences of electronic thermal conductivity (**a**), lattice thermal conductivity (**b**) and total thermal conductivity (**c**) of $Ni_xCo_{4-x}Sb_{12}$ bulks, respectively

conductivity through enhance the phonon scattering. The electrical transport property has been enhanced by Ni doping. The $Ni_{0.3}Co_{3.7}Sb_{12}$ has the highest ZT of 0.52 at 773 K. The new preparation route shows highly competitive compared with the conventional ways both in terms of efficiency and thermoelectric performance.

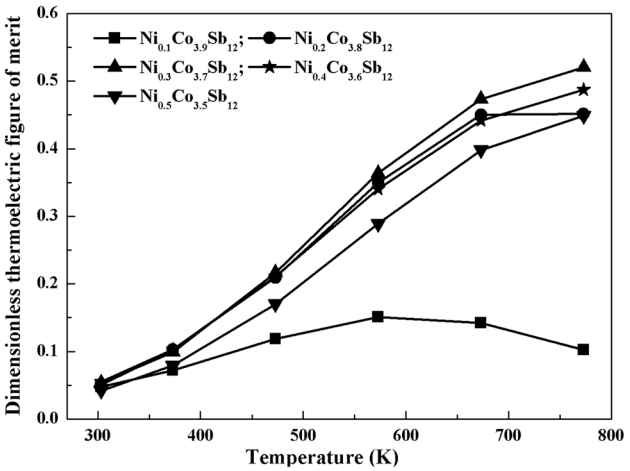

Fig. 7 Thermoelectric figure of merit of $Ni_xCo_{4-x}Sb_{12}$ bulks

Acknowledgements This work was supported by National Natural Science Foundation of China (Grant No. 51574134, No. 51574042), Joint fund between Shenyang National Laboratory for Materials Science and State Key Laboratory of Advanced Processing and Recycling of Nonferrous Metals (Grant No. 18LHPY016) and Anhui university outstanding young talent support program (key project) (Grant No. gxyqZD2017039).

Compliance with ethical standards

Conflict of interest The authors declare that there is no conflict of interest regarding the publication of this paper.

References

1. G. Mahan, B. Sales, J. Sharp, Phys. Today **50**, 42 (1997)
2. G.A. Slack, V.G. Tsoukala, J. Appl. Phys. **76**, 1665 (1994)
3. T. Caillat, A. Borshchevsky, J.P. Fleurial, J. Appl. Phys. **80**, 4442 (1996)
4. G.A. Slack, *CRC Handbook of Thermoelectrics* (CRC Press, Florida, 1995), p. 407
5. B.C. Sales, D. Mandrus, R.K. Williams, Science **272**, 1325 (1996)
6. B.C. Sales, D. Mandrus, B.C. Chakoumakos, Phys. Rev. B **56**, 15081 (1997)
7. J. Yang, D.T. Morelli, G.P. Meisner, W. Chen, J.S. Dyck, C. Uher, Phys. Rev. B **67**, 165207 (2003)
8. X.Y. Li, L.D. Chen, J.F. Fan, W.B. Zhang, T. Kawahara, T. Hirai, J. Appl. Phys. **98**, 4442 (2005)
9. L.D. Dudkin, N.Kh. Abrikosov, Sov. J. Inorg. Chem. **2**, 212 (1957)
10. H. Anno, K. Matsubara, Y. Notohara, T. Sakakibara, H. Tashiro, J. Appl. Phys. **86**, 3780 (1999)
11. J.S. Dyck, W. Chen, J. Yang, G.P. Meisner, C. Uher, Phys. Rev. B **65**, 115204 (2002)
12. H. Kitagawa, M. Wakatsuki, H. Nagaoka, H. Noguchi, Y. Isoda, K. Hasezaki, Y. Noda, J. Phys. Chem. Solids **66**, 1635 (2005)
13. K. Il-Ho, U. Soon-Chul, Met. Mater. Int. **13**, 53 (2007)
14. U. Soon-Chul, K. Il-Ho, J. Korean Phys. Soc. **55**, 942 (2009)
15. H. Qinyu, H. Qing, W. Xiaowei, Y. Jian, L. Yucheng, Y. Xiao, Y. Bo, M. Yi, P. Bed, J. Giri, W. Dezhi, C. Gang, R. Zhifeng, J. Nanosci. Nanotechnol. **8**, 4003 (2008)
16. A. Gharleghi, C.J. Liu, J. Alloy. Compd. **592**, 277 (2014)
17. T. Dahal, H.S. Kim, S. Gahlawat, Acta Mate **117**, 13 (2016)
18. G. Tan, H. Chi, W. Liu, J. Mater. Chem. C **3**, 8372 (2015)
19. S. Wang, J.R. Salvador, J. Yang, NPG Asia Mate **8**, e285 (2016)
20. W.Y. Lai, Q.Q. Chen, Q.Y. He, Q.L. Fan, W. Huang, Chem. Commun. 18(2006)1959
21. Y. He, H.T. Lu, L.M. Sai, W.Y. Lai, Q.L. Fan, L.H. Wang, J. Phys. Chem. B **110**, 13352 (2006)
22. K. Biswas, S. Muir, M.A. Subramanian, Mater. Res. Bull. **46**, 2288 (2011)
23. H.J. Kitchen, S.R. Vallance, J.L. Kennedy, N. Tapia-Ruiz, L. Carassiti, A. Harrison, A.G. Whittaker, T.D. Drysdale, S.W. Kingman, D.H. Gregory, Chem. Rev. **114**, 1170 (2014)
24. Y. Lei, W.S. Gao, Y. Li, R.D. Wan, W. Chen, R. Zheng, L.Q. Ma, H.W. Zhou, Mater. Lett. **233**, 166 (2018)
25. Y. Li, C. Cheng, Y. Lei, M. Wang, R.D. Wan, Dalton Trans. **46**, 33 (2016)
26. Y. Lei, Y. Li, L. Xu, J.Y. Yang, R.D. Wan, H.M. Long, J. Alloy. Compd. **660**, 166 (2016)
27. X. Shi, J. Yang, J.R. Salvador, M. Chi, J.Y. Cho, H. Wang, S.Q. Bai, J. Yang, W.Q. Zhang, L.D. Chen, J. Am. Chem. Soc. **133**, 7837 (2011)
28. Y. Lei, C. Cheng, Y. Li, R.D. Wan, M. Wang, Ceram. Int. **43**, 9343 (2017)
29. Y. Lei, M. Wang, Y. Li, W.S. Gao, R.D. Wan, C. Cheng, Mater. Lett. **201**, 189 (2017)
30. Y. Li, R. Zheng, Y. Lei, W.S. Gao, L.Q. Ma, R.D. Wan, Chin. Pat., 201811362898.1
31. Y. Lei, L.Q. Ma, Y. Li, R.D. Wan, W.S. Gao, R. Zheng, Chin. Pat., 201810812316.9